Studies of $\tau^- \to \eta K^- \nu_\tau$ and $\tau^- \to \eta \pi^- \nu_\tau$ at *BABAR* and a search for a second-class current

P. del Amo Sanchez,[1] J. P. Lees,[1] V. Poireau,[1] E. Prencipe,[1] V. Tisserand,[1] J. Garra Tico,[2] E. Grauges,[2] M. Martinelli,[3a,3b] A. Palano,[3a,3b] M. Pappagallo,[3a,3b] G. Eigen,[4] B. Stugu,[4] L. Sun,[4] M. Battaglia,[5] D. N. Brown,[5] B. Hooberman,[5] L. T. Kerth,[5] Yu. G. Kolomensky,[5] G. Lynch,[5] I. L. Osipenkov,[5] T. Tanabe,[5] C. M. Hawkes,[6] A. T. Watson,[6] H. Koch,[7] T. Schroeder,[7] D. J. Asgeirsson,[8] C. Hearty,[8] T. S. Mattison,[8] J. A. McKenna,[8] A. Khan,[9] A. Randle-Conde,[9] V. E. Blinov,[10] A. R. Buzykaev,[10] V. P. Druzhinin,[10] V. B. Golubev,[10] A. P. Onuchin,[10] S. I. Serednyakov,[10] Yu. I. Skovpen,[10] E. P. Solodov,[10] K. Yu. Todyshev,[10] A. N. Yushkov,[10] M. Bondioli,[11] S. Curry,[11] D. Kirkby,[11] A. J. Lankford,[11] M. Mandelkern,[11] E. C. Martin,[11] D. P. Stoker,[11] H. Atmacan,[12] J. W. Gary,[12] F. Liu,[12] O. Long,[12] G. M. Vitug,[12] C. Campagnari,[13] T. M. Hong,[13] D. Kovalskyi,[13] J. D. Richman,[13] C. West,[13] A. M. Eisner,[14] C. A. Heusch,[14] J. Kroseberg,[14] W. S. Lockman,[14] A. J. Martinez,[14] T. Schalk,[14] B. A. Schumm,[14] A. Seiden,[14] L. O. Winstrom,[14] C. H. Cheng,[15] D. A. Doll,[15] B. Echenard,[15] D. G. Hitlin,[15] P. Ongmongkolkul,[15] F. C. Porter,[15] A. Y. Rakitin,[15] R. Andreassen,[16] M. S. Dubrovin,[16] G. Mancinelli,[16] B. T. Meadows,[16] M. D. Sokoloff,[16] P. C. Bloom,[17] W. T. Ford,[17] A. Gaz,[17] M. Nagel,[17] U. Nauenberg,[17] J. G. Smith,[17] S. R. Wagner,[17] R. Ayad,[18,*] W. H. Toki,[18] H. Jasper,[19] T. M. Karbach,[19] J. Merkel,[19] A. Petzold,[19] B. Spaan,[19] K. Wacker,[19] M. J. Kobel,[20] K. R. Schubert,[20] R. Schwierz,[20] D. Bernard,[21] M. Verderi,[21] P. J. Clark,[22] S. Playfer,[22] J. E. Watson,[22] M. Andreotti,[23a,23b] D. Bettoni,[23a] C. Bozzi,[23a] R. Calabrese,[23a,23b] A. Cecchi,[23a,23b] G. Cibinetto,[23a,23b] E. Fioravanti,[23a,23b] P. Franchini,[23a,23b] E. Luppi,[23a,23b] M. Munerato,[23a,23b] M. Negrini,[23a,23b] A. Petrella,[23a,23b] L. Piemontese,[23a] R. Baldini-Ferroli,[24] A. Calcaterra,[24] R. de Sangro,[24] G. Finocchiaro,[24] M. Nicolaci,[24] S. Pacetti,[24] P. Patteri,[24] I. M. Peruzzi,[24,†] M. Piccolo,[24] M. Rama,[24] A. Zallo,[24] R. Contri,[25a,25b] E. Guido,[25a,25b] M. Lo Vetere,[25a,25b] M. R. Monge,[25a,25b] S. Passaggio,[25a] C. Patrignani,[25a,25b] E. Robutti,[25a] S. Tosi,[25a,25b] B. Bhuyan,[26] V. Prasad,[26] C. L. Lee,[27] M. Morii,[27] A. Adametz,[28] J. Marks,[28] U. Uwer,[28] F. U. Bernlochner,[29] M. Ebert,[29] H. M. Lacker,[29] T. Lueck,[29] A. Volk,[29] P. D. Dauncey,[30] M. Tibbetts,[30] P. K. Behera,[31] U. Mallik,[31] C. Chen,[32] J. Cochran,[32] H. B. Crawley,[32] L. Dong,[32] W. T. Meyer,[32] S. Prell,[32] E. I. Rosenberg,[32] A. E. Rubin,[32] A. V. Gritsan,[33] Z. J. Guo,[33] N. Arnaud,[34] M. Davier,[34] D. Derkach,[34] J. Firmino da Costa,[34] G. Grosdidier,[34] F. Le Diberder,[34] A. M. Lutz,[34] B. Malaescu,[34] A. Perez,[34] P. Roudeau,[34] M. H. Schune,[34] J. Serrano,[34] V. Sordini,[34,‡] A. Stocchi,[34] L. Wang,[34] G. Wormser,[34] D. J. Lange,[35] D. M. Wright,[35] I. Bingham,[36] C. A. Chavez,[36] J. P. Coleman,[36] J. R. Fry,[36] E. Gabathuler,[36] R. Gamet,[36] D. E. Hutchcroft,[36] D. J. Payne,[36] C. Touramanis,[36] A. J. Bevan,[37] F. Di Lodovico,[37] R. Sacco,[37] M. Sigamani,[37] G. Cowan,[38] S. Paramesvaran,[38] A. C. Wren,[38] D. N. Brown,[39] C. L. Davis,[39] A. G. Denig,[40] M. Fritsch,[40] W. Gradl,[40] A. Hafner,[40] K. E. Alwyn,[41] D. Bailey,[41] R. J. Barlow,[41] G. Jackson,[41] G. D. Lafferty,[41] T. J. West,[41] J. Anderson,[42] R. Cenci,[42] A. Jawahery,[42] D. A. Roberts,[42] G. Simi,[42] J. M. Tuggle,[42] C. Dallapiccola,[43] E. Salvati,[43] R. Cowan,[44] D. Dujmic,[44] G. Sciolla,[44] M. Zhao,[44] D. Lindemann,[45] P. M. Patel,[45] S. H. Robertson,[45] M. Schram,[45] P. Biassoni,[46a,46b] A. Lazzaro,[46a,46b] V. Lombardo,[46a] F. Palombo,[46a,46b] S. Stracka,[46a,46b] L. Cremaldi,[47] R. Godang,[47,§] R. Kroeger,[47] P. Sonnek,[47] D. J. Summers,[47] X. Nguyen,[48] M. Simard,[48] P. Taras,[48] G. De Nardo,[49a,49b] D. Monorchio,[49a,49b] G. Onorato,[49a,49b] C. Sciacca,[49a,49b] G. Raven,[50] H. L. Snoek,[50] C. P. Jessop,[51] K. J. Knoepfel,[51] J. M. LoSecco,[51] W. F. Wang,[51] L. A. Corwin,[52] K. Honscheid,[52] R. Kass,[52] J. P. Morris,[52] N. L. Blount,[53] J. Brau,[53] R. Frey,[53] O. Igonkina,[53] J. A. Kolb,[53] R. Rahmat,[53] N. B. Sinev,[53] D. Strom,[53] J. Strube,[53] E. Torrence,[53] G. Castelli,[54a,54b] E. Feltresi,[54a,54b] N. Gagliardi,[54a,54b] M. Margoni,[54a,54b] M. Morandin,[54a] M. Posocco,[54a] M. Rotondo,[54a] F. Simonetto,[54a,54b] R. Stroili,[54a,54b] E. Ben-Haim,[55] G. R. Bonneaud,[55] H. Briand,[55] G. Calderini,[55] J. Chauveau,[55] O. Hamon,[55] Ph. Leruste,[55] G. Marchiori,[55] J. Ocariz,[55] J. Prendki,[55] S. Sitt,[55] M. Biasini,[56a,56b] E. Manoni,[56a,56b] A. Rossi,[56a,56b] C. Angelini,[57a,57b] G. Batignani,[57a,57b] S. Bettarini,[57a,57b] M. Carpinelli,[57a,57b,‖] G. Casarosa,[57a,57b] A. Cervelli,[57a,57b] F. Forti,[57a,57b] M. A. Giorgi,[57a,57b] A. Lusiani,[57a,57c] N. Neri,[57a,57b] E. Paoloni,[57a,57b] G. Rizzo,[57a,57b] J. J. Walsh,[57a] D. Lopes Pegna,[58] C. Lu,[58] J. Olsen,[58] A. J. S. Smith,[58] A. V. Telnov,[58] F. Anulli,[59a] E. Baracchini,[59a,59b] G. Cavoto,[59a] R. Faccini,[59a,59b] F. Ferrarotto,[59a] F. Ferroni,[59a,59b] M. Gaspero,[59a,59b] L. Li Gioi,[59a] M. A. Mazzoni,[59a] G. Piredda,[59a] F. Renga,[59a,59b] T. Hartmann,[60] T. Leddig,[60] H. Schröder,[60] R. Waldi,[60] T. Adye,[61] B. Franek,[61] E. O. Olaiya,[61] F. F. Wilson,[61] S. Emery,[62] G. Hamel de Monchenault,[62] G. Vasseur,[62] Ch. Yèche,[62] M. Zito,[62] M. T. Allen,[63] D. Aston,[63] D. J. Bard,[63] R. Bartoldus,[63] J. F. Benitez,[63] C. Cartaro,[63] M. R. Convery,[63] J. Dorfan,[63] G. P. Dubois-Felsmann,[63] W. Dunwoodie,[63] R. C. Field,[63] M. Franco Sevilla,[63] B. G. Fulsom,[63] A. M. Gabareen,[63] M. T. Graham,[63] P. Grenier,[63] C. Hast,[63] W. R. Innes,[63] M. H. Kelsey,[63] H. Kim,[63] P. Kim,[63] M. L. Kocian,[63] D. W. G. S. Leith,[63] S. Li,[63] B. Lindquist,[63] S. Luitz,[63] V. Luth,[63] H. L. Lynch,[63] D. B. MacFarlane,[63] H. Marsiske,[63] D. R. Muller,[63] H. Neal,[63] S. Nelson,[63] C. P. O'Grady,[63] I. Ofte,[63] M. Perl,[63] T. Pulliam,[63] B. N. Ratcliff,[63]

A. Roodman,[63] A. A. Salnikov,[63] V. Santoro,[63] R. H. Schindler,[63] J. Schwiening,[63] A. Snyder,[63] D. Su,[63] M. K. Sullivan,[63] S. Sun,[63] K. Suzuki,[63] J. M. Thompson,[63] J. Va'vra,[63] A. P. Wagner,[63] M. Weaver,[63] C. A. West,[63] W. J. Wisniewski,[63] M. Wittgen,[63] D. H. Wright,[63] H. W. Wulsin,[63] A. K. Yarritu,[63] C. C. Young,[63] V. Ziegler,[63] X. R. Chen,[64] W. Park,[64] M. V. Purohit,[64] R. M. White,[64] J. R. Wilson,[64] S. J. Sekula,[65] M. Bellis,[66] P. R. Burchat,[66] A. J. Edwards,[66] T. S. Miyashita,[66] S. Ahmed,[67] M. S. Alam,[67] J. A. Ernst,[67] B. Pan,[67] M. A. Saeed,[67] S. B. Zain,[67] N. Guttman,[68] A. Soffer,[68] P. Lund,[69] S. M. Spanier,[69] R. Eckmann,[70] J. L. Ritchie,[70] A. M. Ruland,[70] C. J. Schilling,[70] R. F. Schwitters,[70] B. C. Wray,[70] J. M. Izen,[71] X. C. Lou,[71] F. Bianchi,[72a,72b] D. Gamba,[72a,72b] M. Pelliccioni,[72a,72b] M. Bomben,[73a,73b] L. Lanceri,[73a,73b] L. Vitale,[73a,73b] N. Lopez-March,[74] F. Martinez-Vidal,[74] D. A. Milanes,[74] A. Oyanguren,[74] J. Albert,[75] Sw. Banerjee,[75] H. H. F. Choi,[75] K. Hamano,[75] G. J. King,[75] R. Kowalewski,[75] M. J. Lewczuk,[75] I. M. Nugent,[75] J. M. Roney,[75] R. J. Sobie,[75] T. J. Gershon,[76] P. F. Harrison,[76] T. E. Latham,[76] E. M. T. Puccio,[76] H. R. Band,[77] S. Dasu,[77] K. T. Flood,[77] Y. Pan,[77] R. Prepost,[77] C. O. Vuosalo,[77] and S. L. Wu[77]

(*BABAR* Collaboration)

[1]*Laboratoire d'Annecy-le-Vieux de Physique des Particules (LAPP), Université de Savoie, CNRS/IN2P3, F-74941 Annecy-Le-Vieux, France*
[2]*Universitat de Barcelona, Facultat de Fisica, Departament ECM, E-08028 Barcelona, Spain*
[3a]*INFN Sezione di Bari, I-70126 Bari, Italy*
[3b]*Dipartimento di Fisica, Università di Bari, I-70126 Bari, Italy*
[4]*University of Bergen, Institute of Physics, N-5007 Bergen, Norway*
[5]*Lawrence Berkeley National Laboratory and University of California, Berkeley, California 94720, USA*
[6]*University of Birmingham, Birmingham, B15 2TT, United Kingdom*
[7]*Ruhr Universität Bochum, Institut für Experimentalphysik 1, D-44780 Bochum, Germany*
[8]*University of British Columbia, Vancouver, British Columbia, Canada V6T 1Z1*
[9]*Brunel University, Uxbridge, Middlesex UB8 3PH, United Kingdom*
[10]*Budker Institute of Nuclear Physics, Novosibirsk 630090, Russia*
[11]*University of California at Irvine, Irvine, California 92697, USA*
[12]*University of California at Riverside, Riverside, California 92521, USA*
[13]*University of California at Santa Barbara, Santa Barbara, California 93106, USA*
[14]*University of California at Santa Cruz, Institute for Particle Physics, Santa Cruz, California 95064, USA*
[15]*California Institute of Technology, Pasadena, California 91125, USA*
[16]*University of Cincinnati, Cincinnati, Ohio 45221, USA*
[17]*University of Colorado, Boulder, Colorado 80309, USA*
[18]*Colorado State University, Fort Collins, Colorado 80523, USA*
[19]*Technische Universität Dortmund, Fakultät Physik, D-44221 Dortmund, Germany*
[20]*Technische Universität Dresden, Institut für Kern- und Teilchenphysik, D-01062 Dresden, Germany*
[21]*Laboratoire Leprince-Ringuet, CNRS/IN2P3, Ecole Polytechnique, F-91128 Palaiseau, France*
[22]*University of Edinburgh, Edinburgh EH9 3JZ, United Kingdom*
[23a]*INFN Sezione di Ferrara, I-44100 Ferrara, Italy*
[a23b]*Dipartimento di Fisica, Università di Ferrara, I-44100 Ferrara, Italy*
[24]*INFN Laboratori Nazionali di Frascati, I-00044 Frascati, Italy*
[25a]*INFN Sezione di Genova, I-16146 Genova, Italy*
[25b]*Dipartimento di Fisica, Università di Genova, I-16146 Genova, Italy*
[26]*Indian Institute of Technology Guwahati, Guwahati, Assam, 781 039, India*
[27]*Harvard University, Cambridge, Massachusetts 02138, USA*
[28]*Universität Heidelberg, Physikalisches Institut, Philosophenweg 12, D-69120 Heidelberg, Germany*
[29]*Humboldt-Universität zu Berlin, Institut für Physik, Newtonstrasse 15, D-12489 Berlin, Germany*
[30]*Imperial College London, London, SW7 2AZ, United Kingdom*
[31]*University of Iowa, Iowa City, Iowa 52242, USA*
[32]*Iowa State University, Ames, Iowa 50011-3160, USA*
[33]*Johns Hopkins University, Baltimore, Maryland 21218, USA*
[34]*Laboratoire de l'Accélérateur Linéaire, IN2P3/CNRS et Université Paris-Sud 11, Centre Scientifique d'Orsay, B.P. 34, F-91898 Orsay Cedex, France*
[35]*Lawrence Livermore National Laboratory, Livermore, California 94550, USA*
[36]*University of Liverpool, Liverpool L69 7ZE, United Kingdom*
[37]*Queen Mary, University of London, London, E1 4NS, United Kingdom*
[38]*University of London, Royal Holloway and Bedford New College, Egham, Surrey TW20 0EX, United Kingdom*

[39]*University of Louisville, Louisville, Kentucky 40292, USA*
[40]*Johannes Gutenberg-Universität Mainz, Institut für Kernphysik, D-55099 Mainz, Germany*
[41]*University of Manchester, Manchester M13 9PL, United Kingdom*
[42]*University of Maryland, College Park, Maryland 20742, USA*
[43]*University of Massachusetts, Amherst, Massachusetts 01003, USA*
[44]*Massachusetts Institute of Technology, Laboratory for Nuclear Science, Cambridge, Massachusetts 02139, USA*
[45]*McGill University, Montréal, Québec, Canada H3A 2T8*
[46a]*INFN Sezione di Milano, I-20133 Milano, Italy*
[46b]*Dipartimento di Fisica, Università di Milano, I-20133 Milano, Italy*
[47]*University of Mississippi, University, Mississippi 38677, USA*
[48]*Université de Montréal, Physique des Particules, Montréal, Québec, Canada H3C 3J7*
[49a]*INFN Sezione di Napoli, I-80126 Napoli, Italy*
[49b]*Dipartimento di Scienze Fisiche, Università di Napoli Federico II, I-80126 Napoli, Italy*
[50]*NIKHEF, National Institute for Nuclear Physics and High Energy Physics, NL-1009 DB Amsterdam, The Netherlands*
[51]*University of Notre Dame, Notre Dame, Indiana 46556, USA*
[52]*Ohio State University, Columbus, Ohio 43210, USA*
[53]*University of Oregon, Eugene, Oregon 97403, USA*
[54a]*INFN Sezione di Padova, I-35131 Padova, Italy*
[54b]*Dipartimento di Fisica, Università di Padova, I-35131 Padova, Italy*
[55]*Laboratoire de Physique Nucléaire et de Hautes Energies, IN2P3/CNRS, Université Pierre et Marie Curie-Paris6, Université Denis Diderot-Paris7, F-75252 Paris, France*
[56a]*INFN Sezione di Perugia, I-06100 Perugia, Italy*
[56b]*Dipartimento di Fisica, Università di Perugia, I-06100 Perugia, Italy*
[57a]*INFN Sezione di Pisa, I-56127 Pisa, Italy*
[57b]*Dipartimento di Fisica, Università di Pisa, I-56127 Pisa, Italy*
[57c]*Scuola Normale Superiore di Pisa, I-56127 Pisa, Italy*
[58]*Princeton University, Princeton, New Jersey 08544, USA*
[59a]*INFN Sezione di Roma, I-00185 Roma, Italy*
[59b]*Dipartimento di Fisica, Università di Roma La Sapienza, I-00185 Roma, Italy*
[60]*Universität Rostock, D-18051 Rostock, Germany*
[61]*Rutherford Appleton Laboratory, Chilton, Didcot, Oxon, OX11 0QX, United Kingdom*
[62]*CEA, Irfu, SPP, Centre de Saclay, F-91191 Gif-sur-Yvette, France*
[63]*SLAC National Accelerator Laboratory, Stanford, California 94309 USA*
[64]*University of South Carolina, Columbia, South Carolina 29208, USA*
[65]*Southern Methodist University, Dallas, Texas 75275, USA*
[66]*Stanford University, Stanford, California 94305-4060, USA*
[67]*State University of New York, Albany, New York 12222, USA*
[68]*Tel Aviv University, School of Physics and Astronomy, Tel Aviv, 69978, Israel*
[69]*University of Tennessee, Knoxville, Tennessee 37996, USA*
[70]*University of Texas at Austin, Austin, Texas 78712, USA*
[71]*University of Texas at Dallas, Richardson, Texas 75083, USA*
[72a]*INFN Sezione di Torino, I-10125 Torino, Italy*
[72b]*Dipartimento di Fisica Sperimentale, Università di Torino, I-10125 Torino, Italy*
[73a]*INFN Sezione di Trieste, I-34127 Trieste, Italy*
[73b]*Dipartimento di Fisica, Università di Trieste, I-34127 Trieste, Italy*
[74]*IFIC, Universitat de Valencia-CSIC, E-46071 Valencia, Spain*
[75]*University of Victoria, Victoria, British Columbia, Canada V8W 3P6*
[76]*Department of Physics, University of Warwick, Coventry CV4 7AL, United Kingdom*
[77]*University of Wisconsin, Madison, Wisconsin 53706, USA*
(Received 17 November 2010; published 2 February 2011)

We report on analyses of tau lepton decays $\tau^- \to \eta K^- \nu_\tau$ and $\tau^- \to \eta \pi^- \nu_\tau$, with $\eta \to \pi^+ \pi^- \pi^0$, using 470 fb^{-1} of data from the *BABAR* experiment at PEP-II, collected at center-of-mass energies at and near the $\Upsilon(4S)$ resonance. We measure the branching fraction for the $\tau^- \to \eta K^- \nu_\tau$ decay mode,

*Present address: Temple University, Philadelphia, PA 19122, USA.
†Also with Università di Perugia, Dipartimento di Fisica, Perugia, Italy.
‡Also with Università di Roma La Sapienza, I-00185 Roma, Italy.
§Present address: University of South Alabama, Mobile, AL 36688, USA.
‖Also with Università di Sassari, Sassari, Italy.

$\mathcal{B}(\tau^- \to \eta K^- \nu_\tau) = (1.42 \pm 0.11(\text{stat}) \pm 0.07(\text{syst})) \times 10^{-4}$, and report a 95% confidence level upper limit for the second-class current process $\tau^- \to \eta\pi^- \nu_\tau$, $\mathcal{B}(\tau^- \to \eta\pi^- \nu_\tau) < 9.9 \times 10^{-5}$.

DOI: 10.1103/PhysRevD.83.032002 PACS numbers: 13.35.Dx, 14.60.Fg, 11.30.Ly

I. INTRODUCTION

Weak hadronic currents of spin parity J^P can be classified as either first or second class according to their transformation properties under G parity (a combination of charge conjugation and isospin rotation) [1]. In hadronic τ decays, the first-class currents have $J^{PG} = 0^{++}$, 0^{--}, 1^{+-}, or 1^{-+} and are expected to dominate. The second-class currents, which have $J^{PG} = 0^{+-}$, 0^{-+}, 1^{++}, or 1^{--}, are associated with a matrix element proportional to the mass difference between up and down quarks. They vanish in the limit of perfect isospin symmetry. So, while the standard model does not prohibit second-class currents, such τ decays are expected to have branching fractions of the order of 10^{-5} [2], and no evidence has been found for them to date.

The τ^- lepton provides a clean means to search for second-class currents, through the decay mode $\tau^- \to \eta\pi^- \nu_\tau$ (charge-conjugate reactions are implied throughout this paper). The $\eta\pi^-$ final state must have either $J^{PG} = 0^{+-}$ or $J^{PG} = 1^{--}$, both of which can only be produced via second-class currents. The decay could be mediated by the $a_0(980)^-$ meson or by the $\pi_1(1400)^-$ resonance. The CLEO Collaboration has produced the most stringent limit so far on $\tau^- \to \eta\pi^- \nu_\tau$ decays, finding $\mathcal{B}(\tau^- \to \eta\pi^- \nu_\tau) < 1.4 \times 10^{-4}$ at the 95% confidence level [3]. In this work we search for the $\tau^- \to \eta\pi^- \nu_\tau$ decay, with the η decaying to $\pi^+\pi^-\pi^0$, using the large τ-pair sample available from the *BABAR* experiment.

The $\tau^- \to \eta K^- \nu_\tau$ branching fraction has previously been measured by the CLEO [3], ALEPH [4], and Belle [5] Collaborations, giving a world average value of $\mathcal{B}(\tau^- \to \eta K^- \nu_\tau) = (1.61 \pm 0.11) \times 10^{-4}$ [6]. The measurement of $\mathcal{B}(\tau^- \to \eta K^- \nu_\tau)$ reported here is the first from the *BABAR* experiment, and its consistency with the Particle Data Group value helps to validate the method used for the $\tau^- \to \eta\pi^- \nu_\tau$ analysis.

II. *BABAR* EXPERIMENT

The analysis is based on data recorded by the *BABAR* detector [7] at the PEP-II asymmetric-energy e^+e^- storage rings operated at the SLAC National Accelerator Laboratory. An integrated luminosity of 470 fb^{-1} was collected from e^+e^- annihilations at and near the $\Upsilon(4S)$ resonance: 91% of the luminosity was collected at a center-of-mass energy of $\sqrt{s} = 10.58$ GeV, while 9% was collected 40 MeV below this. With a cross section of (0.919 ± 0.003) nb [8] for τ-pair production at our luminosity-weighted center-of-mass energy, the data sample contains about 432×10^6 produced $\tau^+\tau^-$ events.

The *BABAR* detector is described in detail in Ref. [7]. Charged-particle (track) momenta are measured with a 5-layer double-sided silicon vertex tracker and a 40-layer drift chamber. Outside the drift chamber there is a ring-imaging Cherenkov detector and an electromagnetic calorimeter (EMC) consisting of 6580 CsI(Tl) crystals. These detectors are all inside a superconducting solenoidal magnet that produces a magnetic field of 1.5 T. Outside the magnet there is an instrumented magnetic flux return. In the analysis, electrons are identified from the ratio of calorimeter energy to track momentum (E/p), the shape of the shower in the calorimeter, and the ionization energy loss in the tracking system (dE/dx). Muons are identified by hits in the instrumented magnetic flux return and by their small energy deposits in the calorimeter. Pions and kaons are identified from dE/dx in the tracking system and the Cherenkov angle from the ring-imaging Cherenkov detector. For the selections used in this analysis, pions are positively identified with a typical efficiency of 95% and kaons with an efficiency of 90%. The probability to misidentify a pion as a kaon is typically 1%, while the probability to misidentify a kaon as a pion is about 5%.

III. EVENT SELECTION

Tau pairs are produced back to back in the e^+e^- center-of-mass frame, and so each event is divided into hemispheres using the thrust axis [9], calculated from all reconstructed neutral EMC clusters with an energy above 50 MeV in the laboratory frame and all reconstructed charged particles. Events with four well-reconstructed tracks and zero net charge are selected. Each track is required to have a distance of closest approach to the interaction region of less than 10 cm when projected along the beam axis and less than 1.5 cm in the transverse plane. The events are required to have a ''1–3 topology'' in the center-of-mass frame, where one track is in one hemisphere (the tag hemisphere) and three tracks are in the other hemisphere (the signal hemisphere). The charged particle in the tag hemisphere must be identified as either an electron (e tag) or a muon (μ tag), consistent with coming from a fully leptonic τ decay. Hadronic tags were not used because of the large backgrounds from $e^+e^- \to q\bar{q}$ events.

The τ candidates are reconstructed in the signal hemisphere using the three tracks and a π^0 candidate, which is reconstructed from two separate EMC clusters, each with an energy above 30 MeV in the laboratory frame and not associated with a charged track. The π^0 candidates are required to have an invariant mass within 15 MeV/c^2 of

the nominal π^0 mass [6] and are then fitted to constrain the mass. The π^0 candidates are also required to have an energy in the laboratory frame of at least 200 MeV. Events with exactly one π^0 candidate in the signal hemisphere, where both EMC clusters are also in the signal hemisphere, are selected.

Backgrounds arise from a number of sources, including $e^+e^- \to q\bar{q}$ events (where $q = usdc$) that contain η mesons, and τ-pair events in which a τ decays into a channel containing an η meson. The latter category includes $\tau^- \to \eta\pi^-\pi^0\nu_\tau$, $\tau^- \to \eta K^0\pi^-\nu_\tau$, $\tau^- \to \eta K^-\pi^0\nu_\tau$, and $\tau^- \to \eta K^-\nu_\tau$ (background for the $\tau^- \to \eta\pi^-\nu_\tau$ mode). These modes contribute background events when π^0 or K^0_L mesons are missing or when pions or kaons are misidentified.

To reduce backgrounds a number of other selections are applied. The $e^+e^- \to q\bar{q}$ events are suppressed by requiring the total visible energy of the event in the lab frame to be less than 80% of the initial-state energy (τ-pair events have missing energy carried by neutrinos). This background is also suppressed by requiring the magnitude of the event thrust in the center-of-mass frame to be greater than 0.95 (τ-pair events at *BABAR* are highly collinear). The cosine of the angle between the thrust axis and the beam axis is required to be less than 0.8 to ensure the selected events are well-reconstructed, without particles passing through the edges of the active detector region near the beam pipe. To reduce τ background modes containing extra π^0 particles or K^0_L mesons, events are rejected if they have any additional neutral EMC clusters in the signal hemisphere with energy above 100 MeV in the laboratory frame. After all selections, background from $b\bar{b}$ events is negligible, due mainly to the effects of the cuts on the event multiplicity and thrust.

The overall strategy for the analysis is to fit the $\pi^+\pi^-\pi^0$ mass spectra from $\tau^- \to \pi^+\pi^-\pi^0 K^-\nu_\tau$ and $\tau^- \to \pi^+\pi^-\pi^0\pi^-\nu_\tau$ candidate events, to determine the numbers of $\eta \to \pi^+\pi^-\pi^0$ decays in the selected samples. Monte Carlo event samples are used to estimate the numbers of η mesons expected from the background modes, thus allowing the contribution from the signal modes to be determined.

The largest source of combinatorial background in the 3π mass spectra comes from the $\tau^- \to \pi^+\pi^-\pi^0\pi^-\nu_\tau$ channel, which is dominated by $\omega(782)\pi^-\nu_\tau$, with a significant $\rho(770)\pi\pi\nu_\tau$ contribution. In addition, there is a small background in the e-tag sample from Bhabha events. To avoid any model dependence in the analyses, no additional cuts are used to remove these backgrounds, since such cuts would distort the ηK^- and $\eta\pi^-$ mass spectra.

IV. MONTE CARLO SIMULATIONS

Monte Carlo (MC) simulations are used to measure the signal efficiencies as well as the levels of background. The production of τ pairs is simulated with the KK2F generator [10], and the decays of the τ lepton are modeled with TAUOLA [11]. In addition to samples of τ-pair events in which the τ leptons decay according to known branching fractions, samples of τ pairs are produced for the main τ background modes and for the signal modes. In these dedicated samples, one τ in each event is decayed through the specified mode and the other decays according to Particle Data Group branching fractions.

Continuum $q\bar{q}$ events are separated into two samples: one for $u\bar{u}$, $d\bar{d}$, and $s\bar{s}$ (the uds sample) and another for $c\bar{c}$ (the $c\bar{c}$ sample). Both samples are simulated using JETSET [12], with EVTGEN [13] used to simulate the decays of charmed particles. Production of $\Upsilon(4S)$ events and B meson decays are simulated using EVTGEN. Final-state radiative effects are simulated using PHOTOS [14].

The detector response is modeled with GEANT4 [15], and the MC events are fully reconstructed and analyzed in the same manner as the data.

V. ANALYSIS

A. The $\pi^+\pi^-\pi^0$ mass spectra

In the analysis, all three charged particles in the signal hemisphere are initially assumed to be pions, with no requirements on the particle identification (PID) selectors. Each event therefore has two possible $\pi^+\pi^-\pi^0$ combinations. The remaining track associated with each combination in the signal hemisphere is referred to as the "bachelor" track.

For the $\tau^- \to \eta K^-\nu_\tau$ analysis, the bachelor track must be identified as a kaon and the $\pi^+\pi^-\pi^0 K^-$ mass is required to be less than the τ mass. The $\pi^+\pi^-\pi^0$ mass spectra with these selections are shown in Fig. 1 separately for the e-tag and the μ-tag samples; clear η peaks are visible in both spectra. The curves in Fig. 1 show the results of fits described in Sec. V C.

The ηK^- mass distribution, as shown in Fig. 2, is constructed using a sideband subtraction method whereby the $\pi^+\pi^-\pi^0 K^-$ mass spectrum for 3π mass in the η sideband regions (0.510–0.525 and 0.570–0.585 GeV/c^2) is subtracted from the spectrum where the 3π mass lies in the η peak region (0.54–0.555 GeV/c^2). To correct for the shape of the combinatorial background, the entries for the sideband region are weighted according to factors found by integrating over the background functions (discussed in Sec. V C) from the fitted $\pi^+\pi^-\pi^0$ mass spectra. For this figure, the various MC samples (see Sec. IV) are combined according to expected cross sections and the overall sample is normalized to the data luminosity. The results show agreement between data and MC simulations, indicating that the $\tau^- \to \eta K^-\nu_\tau$ decay mode, which dominates the distribution, is adequately modeled in TAUOLA.

In the search for $\tau^- \to \eta\pi^-\nu_\tau$ decays, the bachelor track must be identified as a pion and the $\pi^+\pi^-\pi^0\pi^-$ mass is required to be less than the τ mass. The resulting $\pi^+\pi^-\pi^0$ mass spectra are shown in Fig. 3, again

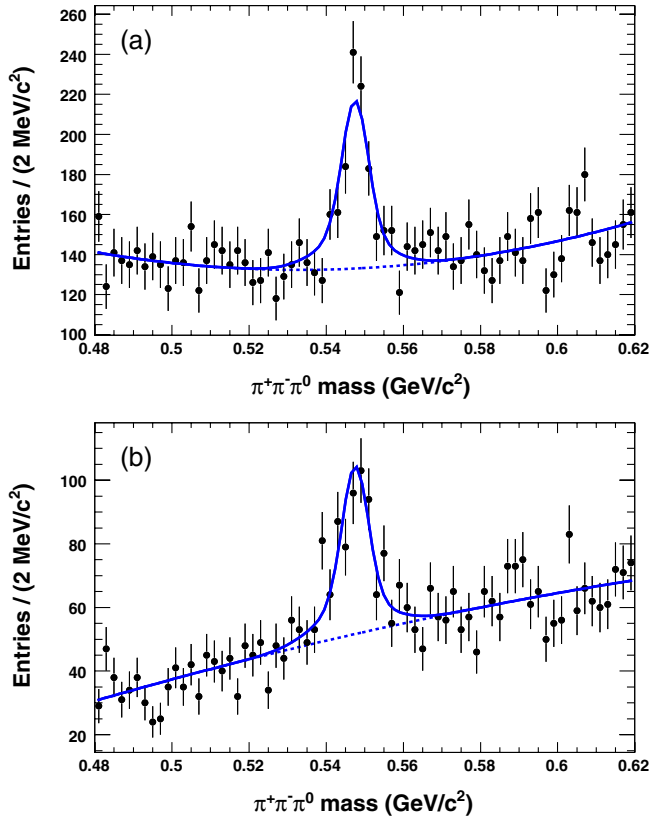

FIG. 1 (color online). Mass spectra for $\pi^+\pi^-\pi^0$ in $\tau^- \to \pi^+\pi^-\pi^0 K^-\nu_\tau$ candidates, for (a) e-tag data and (b) μ-tag data. The curves show the results of the fits described in the text. Note the suppressed zero on the y axes.

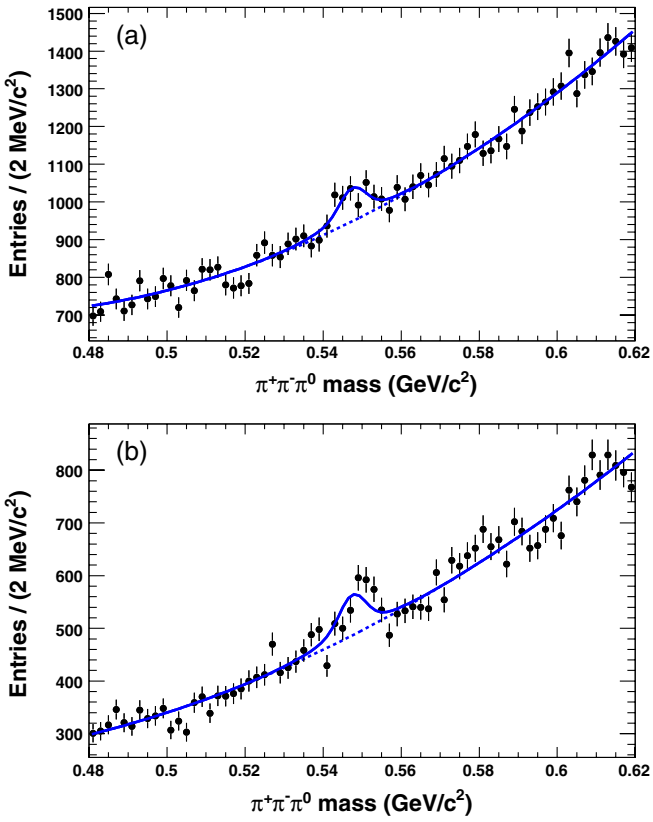

FIG. 3 (color online). Invariant $\pi^+\pi^-\pi^0$ mass distributions for $\tau^- \to \pi^+\pi^-\pi^0\pi^-\nu_\tau$ candidates, for (a) e-tag data (b) μ-tag data. The curves show the results of the fits described in the text. Note the suppressed zero on the y axes.

separately for e-tag and μ-tag events. It should be noted that while the signal $\tau^- \to \eta K^-\nu_\tau$ channel contributes over 90% to the η peaks in Fig. 1, the peaks in Fig. 3 come largely or exclusively from backgrounds to the $\tau^- \to \eta\pi^-\nu_\tau$ search (as shown in Tables I and II, to be discussed below). Figure 4 shows the $\eta\pi$ mass distribution, constructed using the sideband subtraction method, as described above.

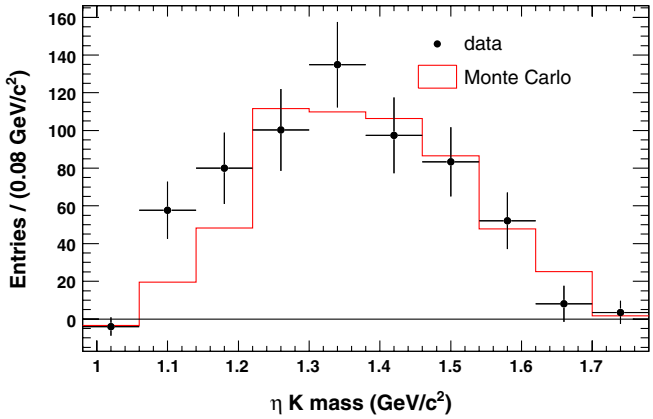

FIG. 2 (color online). The ηK^- mass distributions for the data and MC samples, for e- and μ-tag events, obtained from the sideband subtraction method as described in the text. The MC samples are normalized to the data luminosity; in particular, the $\tau^- \to \eta K^-\nu_\tau$ sample is normalized to luminosity with the branching fraction reported in this paper.

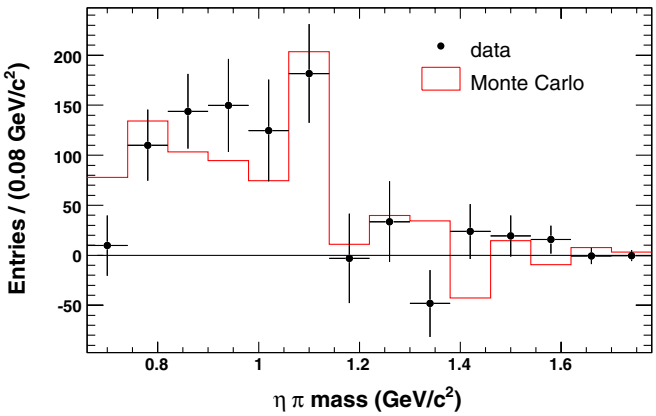

FIG. 4 (color online). The $\eta\pi^-$ mass distributions for the data and MC samples, for e- and μ-tag events, obtained from the sideband subtraction method as described in the text. The MC samples are normalized to the data luminosity; in particular, there are no $\tau^- \to \eta\pi^-\nu_\tau$ MC events.

B. Fit parameters for the η peaks

To study the shapes of the η peaks in data and MC simulations, high-statistics samples are examined. The high-statistics MC sample comprises the sum of e- and μ-tagged events from the dedicated $\tau^- \to \eta\pi^-\nu_\tau$ sample that are selected as $\tau^- \to \pi^+\pi^-\pi^0\pi^-\nu_\tau$ candidates and the e- and μ-tagged events from the dedicated $\tau^- \to \eta K^-\nu_\tau$ sample that are selected as $\tau^- \to \pi^+\pi^-\pi^0 K^-\nu_\tau$ candidates. For the data, we define a high-statistics control sample by replacing the electron and muon tags with a charged pion tag and loosening the selection criteria on the thrust magnitude and total event energy. The high-statistics control sample then comprises all those events that are selected to be $\tau^- \to \pi^+\pi^-\pi^0\pi^-\nu_\tau$ candidates or $\tau^- \to \pi^+\pi^-\pi^0 K^-\nu_\tau$ candidates. The control sample thus defined contains a factor of 20 more $\eta \to \pi^+\pi^-\pi^0$ decays than the standard data sample, coming mainly from *uds* events.

The shapes of the η peaks in both data and MC simulations are found to be well described by double-Gaussian functions. Each double-Gaussian function has five parameters: two peak masses, two widths, and a relative contribution from each Gaussian peak. The values of these parameters are determined in fits to the high-statistics samples and are then fixed in the fits to the signal-candidate data (Figs. 1 and 3) and MC samples. For the data sample, the core Gaussian has a width of (3.4 ± 0.1) MeV$/c^2$ and a relative contribution of $62 \pm 4\%$. For the MC sample, the core Gaussian has a width of (3.8 ± 0.1) MeV$/c^2$ and a relative contribution of $71 \pm 2\%$.

C. Fits to the mass spectra

To measure the number of η mesons in the data and MC samples, the $\pi^+\pi^-\pi^0$ mass spectra are fitted over the range 0.48–0.62 GeV$/c^2$ using a binned maximum likelihood fit. The background is modeled as a second-order polynomial while the η peak is modeled using the double-Gaussian function. The number of events in the η peak is a free parameter in the fits, while the five parameters of the double-Gaussian function are fixed to the values obtained by fitting to the high-statistics samples, as described above. The fit results and errors are given in Tables I and II, which are discussed later in Sec. VI.

D. Efficiency

The efficiency to reconstruct a signal event is defined as the probability that a genuine signal event contributes an entry to the fitted η peak. The $\pi^+\pi^-\pi^0$ mass spectra from the dedicated $\tau^- \to \eta\pi^-\nu_\tau$ and $\tau^- \to \eta K^-\nu_\tau$ MC samples are fitted to measure the number of reconstructed η mesons in each sample. The $\tau^- \to \eta K^-\nu_\tau$ efficiency is found to be $0.336 \pm 0.003\%$ for e-tag and $0.242 \pm 0.003\%$ for μ-tag events, giving a total efficiency of $0.578 \pm 0.004\%$. For $\tau^- \to \eta\pi^-\nu_\tau$ the corresponding values are $0.286 \pm 0.004\%$, $0.186 \pm 0.004\%$, and $0.472 \pm 0.006\%$. The efficiency for the $\tau^- \to \eta K^-\nu_\tau$ mode is higher mainly because of a higher efficiency for the cut on the thrust magnitude.

VI. BACKGROUNDS

As listed in Sec. IV, background sources of η mesons include $q\bar{q}$ events as well as τ decay modes that contain η mesons, such as $\tau^- \to \eta\pi^-\pi^0\nu_\tau$, $\tau^- \to \eta K^-\pi^0\nu_\tau$, and $\tau^- \to \eta K^0\pi^-\nu_\tau$. To measure the branching fractions of $\tau^- \to \eta K^-\nu_\tau$ and $\tau^- \to \eta\pi^-\nu_\tau$, the numbers of η mesons obtained from the fits must be corrected for contributions from the background channels.

The number of $\eta \to \pi^+\pi^-\pi^0$ decays contributed by each background mode is estimated from the MC samples, as discussed further below, and the results are summarized in Tables I and II, where the first errors are statistical and the second are systematic (the systematic errors come from the uncertainties on branching fractions).

A. Background from *uds* events

Since inclusive η production in *uds* events at *BABAR* energies has not been well measured and may be poorly simulated in the JETSET Monte Carlo simulation, the high-statistics data control samples, described above, are used to correct the MC samples for the level of background from this source.

To correct the *uds* simulation to better match the data, scaling factors are evaluated based on ratios of the numbers of reconstructed η mesons in the high-statistics (*uds*-enriched) data and MC samples. The scaling factors

TABLE I. The numbers of η mesons, for ηK^- candidates, that are expected to come from each background mode and the total number of η mesons seen in the data sample, as explained in Secs. VI and VII. For each entry, the first error is statistical and the second error is systematic.

Background contribution	Expected number of events e-tag	μ-tag
uds	$4.5 \pm 2.7 \pm 2.3$	$8.9 \pm 4.7 \pm 4.5$
$c\bar{c}$	$13.8 \pm 8.3 \pm 3.5$	$0.7 \pm 5.5 \pm 0.2$
$\tau^- \to \eta\pi^-\pi^0\nu_\tau$	$13.3 \pm 3.7 \pm 0.7$	$2.9 \pm 2.0 \pm 0.2$
$\tau^- \to \eta K^-\pi^0\nu_\tau$	$8.4 \pm 0.5 \pm 2.1$	$5.0 \pm 0.4 \pm 1.3$
$\tau^- \to \eta K^0\pi^-\nu_\tau$	$3.9 \pm 0.5 \pm 0.7$	$2.3 \pm 0.4 \pm 0.4$
Total background	$44 \pm 10 \pm 5$	$20 \pm 8 \pm 5$
Combined e- and μ-tag	$64 \pm 12 \pm 8$	
Measured in data	Number of events in data	
	$463 \pm 44 \pm 12$	$291 \pm 30 \pm 10$
Combined e- and μ-tag	$754 \pm 53 \pm 16$	
Signal	Measured data minus background	
	$419 \pm 44 \pm 16$	$271 \pm 30 \pm 13$
Combined e- and μ-tag	$690 \pm 53 \pm 22$	

TABLE II. The numbers of η mesons, for $\eta\pi^-$ candidates, that are expected to come from each background mode and the total number of η mesons seen in the data sample, as explained in Secs. VI and VII. For each entry, the first error is statistical and the second error is systematic.

Background contribution	Expected number of events *e*-tag	μ-tag
uds	$20 \pm 9 \pm 14$	$64 \pm 13 \pm 43$
$c\bar{c}$	$74 \pm 20 \pm 19$	$54 \pm 15 \pm 13$
$\tau^- \to \eta\pi^-\pi^0\nu_\tau$	$215 \pm 14 \pm 12$	$118 \pm 11 \pm 7$
$\tau^- \to \eta K^0\pi^-\nu_\tau$	$100 \pm 2 \pm 17$	$71 \pm 2 \pm 12$
$\tau^- \to \eta K^-\nu_\tau$	$35 \pm 1 \pm 2$	$26 \pm 1 \pm 1$
$\tau^- \to \eta K^-\pi^0\nu_\tau$	$0.6 \pm 0.2 \pm 0.1$	$0.2 \pm 0.2 \pm 0.1$
Total background	$445 \pm 27 \pm 31$	$333 \pm 23 \pm 47$
Combined *e*- and μ-tag	$778 \pm 35 \pm 73$	
Measured in data	Number of events in data	
	$489 \pm 111 \pm 15$	$424 \pm 74 \pm 13$
Combined *e*- and μ-tag	$913 \pm 134 \pm 20$	
Signal	Measured data minus background	
	$44 \pm 111 \pm 43$	$91 \pm 74 \pm 54$
Combined *e*- and μ-tag	$135 \pm 134 \pm 83$	

are found to be 1.0 ± 0.5 for the ηK^- channel and 1.5 ± 1.0 for the $\eta\pi^-$ channel. The relatively large uncertainty for the scaling factor in the $\eta\pi^-$ channel is a reflection of the poor simulation of $a_0 \to \eta\pi^-$ production in uds events.

B. Background from $c\bar{c}$ events

The simulation of η meson production in $c\bar{c}$ events is more reliable than in uds events, since $c\bar{c}$ events always contain two charmed particles, whose branching fractions are well known [6]. To calculate a $c\bar{c}$ scaling factor, $\tau^- \to \pi^+\pi^-\pi^0\pi^-\nu_\tau$ candidates are selected from the *e*- and μ-tagged samples. To enhance the number of $c\bar{c}$ events the selection made on the thrust magnitude is removed and events with a $\pi^+\pi^-\pi^0\pi^-$ mass greater than the τ mass are selected.

The $\eta\pi^-$ mass distribution is constructed using the sideband subtraction method described above. Peaks are observed that correspond to the $D^- \to \eta\pi^-$ and $D_s^- \to \eta\pi^-$ decays. A scaling factor of 1.2 ± 0.3 is found to give best agreement between data and MC simulations in the numbers of D^- and D_s^- mesons. Although there is no evidence for poor simulation of η production in $c\bar{c}$ events, this is conservatively chosen as the $c\bar{c}$ scaling factor for the $\pi^+\pi^-\pi^0K^-$ and $\pi^+\pi^-\pi^0\pi^-$ analyses.

C. Background from τ decays

The numbers of η mesons in the dedicated MC samples for each background τ-decay mode are calculated by fitting the $\pi^+\pi^-\pi^0$ mass spectra as previously described. These numbers, together with the numbers of events before selections are made, the luminosities of the data, and the known branching fractions [6], are used to calculate the numbers of η mesons in the data sample that are expected to come from each background mode.

D. Uncertainties on backgrounds

For each background mode included in Tables I and II there is a statistical error, which comes from the fits to the $\pi^+\pi^-\pi^0$ mass spectra arising mainly from limited MC statistics, and a systematic error from uncertainties in branching fractions or scaling factors. When combining the *e*-tag and μ-tag samples, correlated errors (e.g. due to branching fraction uncertainties) are taken into account. The total statistical and systematic errors are combined in quadrature and propagated as systematic errors on the final measurements.

VII. RESULTS AND CONCLUSION

Tables I and II give the numbers of η mesons measured in data, as obtained from the fits (Sec. V C), for the ηK^- and $\eta\pi^-$ candidate samples. The first errors are statistical, while the second are systematic, calculated by varying the values of the fixed parameters within their uncertainties. In both channels, the *e*-tag and μ-tag analyses are combined for the final phase of the analyses.

The fits to the ηK^- data sample yield $754 \pm 53 \pm 16$ η mesons, compared to an expected background of $64 \pm 12 \pm 8$, giving a signal contribution of $690 \pm 53 \pm 22$ η mesons. For the $\eta\pi^-$ sample, the fits yield $913 \pm 134 \pm 20$ η mesons, with an expected background of $778 \pm 35 \pm 73$, and a signal contribution of $135 \pm 134 \pm 83$ η mesons. The statistical errors on the signals are taken to be the same as those on the unsubtracted measurements, and the other error contributions are combined to give the total systematic errors.

Additional sources of systematic uncertainties on the measurements of branching fractions are listed in Table III. The uncertainty in the π^0 detection efficiency is 3% per π^0 candidate, while the uncertainty on the tracking efficiency for charged particles is 0.5% per track, which is added linearly for the four tracks. The error on the efficiency due to MC statistics comes from the statistical error on the fits, as given in Sec. V D. The uncertainties on the PID selectors are calculated from control samples to be 0.7% for electrons, 1.8% for muons, 1.2% for kaons, and 0.2% for pions. The uncertainty on the number of $\tau^+\ \tau^-$ events is 0.9%.

The branching fraction for $\tau^- \to \eta K^-\nu_\tau$ is measured to be

$$\mathcal{B}(\tau^- \to \eta K^-\nu_\tau) = (1.42 \pm 0.11(\text{stat}) \pm 0.07(\text{syst})) \times 10^{-4}. \quad (1)$$

TABLE III. Additional systematic uncertainties on the $\tau^- \to \eta K^- \nu_\tau$ and $\tau^- \to \eta \pi^- \nu_\tau$ branching fractions.

	$\tau^- \to \eta K^- \nu_\tau$			$\tau^- \to \eta \pi^- \nu_\tau$		
Source	e-tag	μ-tag	e- and μ-tag	e-tag	μ-tag	e- and μ-tag
π^0 efficiency	3.0%	3.0%	3.0%	3.0%	3.0%	3.0%
Tracking efficiency	2.0%	2.0%	2.0%	2.0%	2.0%	2.0%
Error on efficiency due to MC statistics	1.0%	1.1%	0.7%	1.6%	1.9%	1.2%
e-tag, μ-tag PID	0.7%	1.8%	1.1%	0.7%	1.8%	1.1%
Bachelor K^-/π^- PID	1.2%	1.2%	1.2%	0.2%	0.2%	0.2%
Luminosity and $\sigma_{\tau^+\tau^-}$	0.9%	0.9%	0.9%	0.9%	0.9%	0.9%
Total systematic uncertainty	4.1%	4.4%	4.1%	4.1%	4.6%	4.1%

The values obtained separately for the e-tag and μ-tag samples are $(1.48 \pm 0.15 \pm 0.08) \times 10^{-4}$ and $(1.33 \pm 0.15 \pm 0.09) \times 10^{-4}$, respectively. The measurement is compatible with the world average of $(1.61 \pm 0.11) \times 10^{-4}$, which is dominated by the Belle measurement of $(1.58 \pm 0.05 \pm 0.09) \times 10^{-4}$ [5]; this Belle measurement used the $\eta \to \gamma\gamma$ and the $\eta \to \pi^+\pi^-\pi^0$ decay modes [a branching fraction of $(1.60 \pm 0.15 \pm 0.10) \times 10^{-4}$ is reported from the $\eta \to \pi^+\pi^-\pi^0$ decay mode alone]. The Belle Collaboration suggest that previous $\tau^- \to \eta K^- \nu_\tau$ measurements [3,4] underestimated background contamination, an assertion that is supported by the observation that the Belle and *BABAR* results are in good agreement. The weighted average of the *BABAR* and Belle results is

$$\mathcal{B}(\tau^- \to \eta K^- \nu_\tau) = (1.52 \pm 0.08) \times 10^{-4}, \quad (2)$$

where small correlations between the systematic uncertainties of the two experiments have not been taken into account.

The branching fraction for $\tau^- \to \eta \pi^- \nu_\tau$ is measured to be

$$\mathcal{B}(\tau^- \to \eta \pi^- \nu_\tau) = (3.4 \pm 3.4(\text{stat}) \pm 2.1(\text{syst})) \times 10^{-5}. \quad (3)$$

With no evidence for a signal, a 95% confidence level upper limit is obtained using $\mathcal{B} + 1.645\sigma$, where $\mathcal{B}$ is the measured $\tau^- \to \eta \pi^- \nu_\tau$ branching fraction and σ is its total uncertainty. We find

$$\mathcal{B}(\tau^- \to \eta \pi^- \nu_\tau) < 9.9 \times 10^{-5}. \quad (4)$$

The limit at 90% confidence level is $\mathcal{B}(\tau^- \to \eta \pi^- \nu_\tau) < 8.5 \times 10^{-5}$. This limit improves on the CLEO value [3], further constraining branching fractions for second-class current processes.

ACKNOWLEDGMENTS

We are grateful for the extraordinary contributions of our PEP-II colleagues in achieving the excellent luminosity and machine conditions that have made this work possible. The success of this project also relies critically on the expertise and dedication of the computing organizations that support *BABAR*. The collaborating institutions wish to thank SLAC for its support and the kind hospitality extended to them. This work is supported by the U.S. Department of Energy and National Science Foundation, the Natural Sciences and Engineering Research Council (Canada), the Commissariat à l'Energie Atomique and Institut National de Physique Nucléaire et de Physique des Particules (France), the Bundesministerium für Bildung und Forschung and Deutsche Forschungsgemeinschaft (Germany), the Istituto Nazionale di Fisica Nucleare (Italy), the Foundation for Fundamental Research on Matter (The Netherlands), the Research Council of Norway, the Ministry of Education and Science of the Russian Federation, Ministerio de Ciencia e Innovación (Spain), and the Science and Technology Facilities Council (United Kingdom). Individuals have received support from the Marie-Curie IEF program (European Union), the A. P. Sloan Foundation (USA), and the Binational Science Foundation (U.S.–Israel).

[1] S. Weinberg, Phys. Rev. **112**, 1375 (1958).
[2] A. Pich, Phys. Lett. B **196**, 561 (1987); S. Nussinov and A. Soffer, Phys. Rev. D **78**, 033006 (2008).
[3] J. Bartelt *et al.* (CLEO Collaboration), Phys. Rev. Lett. **76**, 4119 (1996).
[4] D. Buskulic *et al.* (ALEPH Collaboration), Z. Phys. C **74**, 263 (1997).
[5] K. Inami *et al.* (Belle Collaboration), Phys. Lett. B **672**, 209 (2009).
[6] K. Nakamura *et al.* (Particle Data Group), J. Phys. G **37**, 075021 (2010).
[7] B. Aubert *et al.* (*BABAR* Collaboration), Nucl. Instrum. Methods Phys. Res., Sect. A **479**, 1 (2002).

[8] S. Banerjee, B. Pietrzyk, J. M. Roney, and Z. Was, Phys. Rev. D **77**, 054012 (2008).
[9] S. Brandt *et al.*, Phys. Lett. **12**, 57 (1964); E. Farhi, Phys. Rev. Lett. **39**, 1587 (1977).
[10] B. F. Ward, S. Jadach, and Z. Was, Nucl. Phys. B, Proc. Suppl. **116**, 73 (2003).
[11] S. Jadach, Z. Was, R. Decker, and J. H. Kuhn, Comput. Phys. Commun. **76**, 361 (1993).
[12] T. Sjostrand, Comput. Phys. Commun. **82**, 74 (1994).
[13] D. J. Lange, Nucl. Instrum. Methods Phys. Res., Sect. A **462**, 152 (2001).
[14] E. Barberio and Z. Was, Comput. Phys. Commun. **79**, 291 (1994).
[15] S. Agostinelli *et al.* (GEANT4 Collaboration), Nucl. Instrum. Methods Phys. Res., Sect. A **506**, 250 (2003).